

## Superconductivity at the $\text{LaAlO}_3/\text{SrTiO}_3$ interface

This article has been downloaded from IOPscience. Please scroll down to see the full text article.

2009 J. Phys.: Condens. Matter 21 164213

(<http://iopscience.iop.org/0953-8984/21/16/164213>)

View [the table of contents for this issue](#), or go to the [journal homepage](#) for more

Download details:

IP Address: 129.252.86.83

The article was downloaded on 29/05/2010 at 19:09

Please note that [terms and conditions apply](#).

# Superconductivity at the LaAlO<sub>3</sub>/SrTiO<sub>3</sub> interface

S Gariglio, N Reyren, A D Caviglia and J-M Triscone

DPMC, University of Geneva, 24 Quai E.-Ansermet 1211 Genève 4, Switzerland

E-mail: [stefano.gariglio@unige.ch](mailto:stefano.gariglio@unige.ch)

Received 22 January 2009

Published 31 March 2009

Online at [stacks.iop.org/JPhysCM/21/164213](http://stacks.iop.org/JPhysCM/21/164213)

## Abstract

We report on the structural characterization of LaAlO<sub>3</sub>/SrTiO<sub>3</sub> interfaces and on their transport properties. LaAlO<sub>3</sub> films were prepared using pulsed laser deposition onto TiO<sub>2</sub> terminated (001) SrTiO<sub>3</sub> substrates inducing a metallic conduction at the interface. Resistance and Hall effect measurements reveal a sheet carrier density between 0.4 and  $1.2 \times 10^{14}$  electrons cm<sup>-2</sup> at room temperature and a mobility of  $\sim 300$  cm<sup>2</sup> V<sup>-1</sup> s<sup>-1</sup> at low temperatures. A transition to a superconducting state is observed at a temperature of  $\sim 200$  mK. The superconducting characteristics display signatures of 2D superconductivity.

(Some figures in this article are in colour only in the electronic version)

## 1. Introduction

Ohtomo and Hwang discovered in 2004 that metallic conduction occurs at the interface between two insulating materials, LaAlO<sub>3</sub> (LAO) and SrTiO<sub>3</sub> (STO) [1]. This discovery has generated a lot of interest and motivated extensive theoretical and experimental work aimed at investigating the physics of complex oxide interfaces. In such systems, novel electronic properties have been predicted [2] and recently observed [3, 4]. In the specific case of the LAO/STO interface, magnetic effects [5], superconductivity [6] and a rich electronic phase diagram [7] have been reported. The mechanism leading to the formation of a mobile electron gas at the LAO/STO interface remains today a highly debated issue. A possible explanation is the so-called ‘polar catastrophe’ scenario. According to this interpretation, the origin of this phenomenon is linked to a polar discontinuity occurring at the LAO/STO interface between the polar (001) LAO atomic planes and non-polar (001) STO planes [8]. When the polar LAO atomic planes are stacked on top of each other, an electric potential develops as the film thickness increases. Above a critical thickness, an electronic reconstruction may take place leading to a charge transfer at the interface, reducing the electrostatic energy and creating a two-dimensional electron gas. Experimental evidence supporting this scenario has been reported in reference [9], where the electron gas and metallic conduction have only been observed for LAO films at least 4 unit cells (u.c.) thick. The confinement of the electron gas has been estimated

from analyses of the superconducting properties [10] and by room temperature conductive atomic force measurements [11]. These experiments lead to an estimate of the thickness of the electron gas of a few nanometers. In this short paper we report on the structural characterization of LAO/STO structures and describe their transport properties in the normal and superconducting states. We analyze the superconducting behavior in the framework of the Berezinskii–Kosterlitz–Thouless (BKT) theory of 2D superconductivity.

## 2. Experimental details

Conducting interfaces were prepared by depositing more than 3 u.c. of LAO on top of (001) SrTiO<sub>3</sub> single crystals with TiO<sub>2</sub>-terminated surfaces. The films were grown by pulsed laser deposition (PLD) at 800 °C in  $1 \times 10^{-4}$  mbar of O<sub>2</sub> with a repetition rate of 1 Hz. The fluence of each laser pulse was 0.6 J cm<sup>-2</sup>. After the LAO deposition, each sample was annealed in 200 mbar of O<sub>2</sub> at about 600 °C for one hour and cooled down to room temperature in the same O<sub>2</sub> background pressure. The growth was monitored *in situ* using reflection high energy electron diffraction (RHEED), which allows a control of the thickness with sub-u.c. precision [12]. Samples with different thicknesses of LAO were systematically characterized, analyzing the surface morphology by atomic force microscopy (AFM) and crystalline quality by x-ray diffraction (XRD). The samples were then patterned in a geometry suitable for four point transport measurements. The patterning technique is based on the fact that only regions

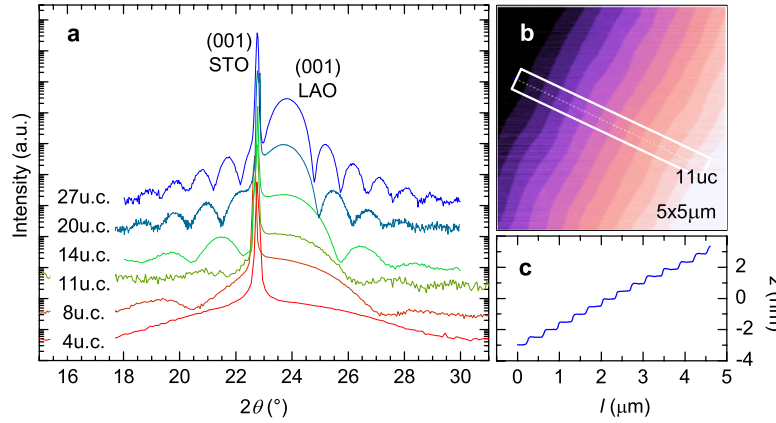


**Figure 1.** Structural characterization of LAO thin films. (a) X-ray  $\theta$ - $2\theta$  diffractograms around the (001) LAO and STO reflections for LAO thin films with different thicknesses. (b) AFM topography performed on an 11 u.c. LAO thick film and (c) a height profile averaged over the width of the area delimited by the white lines. The step-and-terrace structure reflecting the miscut of the STO substrate is clearly visible.

covered by more than 3 u.c. are conducting [9]. The LAO thickness was thus reduced using argon ion milling down to 2 u.c. in specific regions of the samples while protecting the transport channels with photoresist. Once the conducting channels were defined, the transport properties were investigated in a dilution cryostat.

### 3. Results

Figure 1(a) displays  $\theta$ - $2\theta$  x-ray diffractograms close to the (001) LAO and STO reflections for samples with different LAO thicknesses. As can be seen in the figure, the period of finite size Fresnel oscillations around the diffraction peak changes with the LAO film thickness and allows the thickness of the LAO layer to be determined. The thickness obtained from the XRD data analyses is found to agree within one unit cell with the thickness deduced from the RHEED intensity oscillations. Figure 1(b) shows a typical AFM topography measured on an 11 u.c. LAO sample. We observe that the step-and-terrace structure of the substrate is reproduced on the surface of the film. The step height is about 4 Å, corresponding to 1 u.c. of LAO, as shown in figure 1(c).

Reciprocal space maps (RSMs) were made to inspect the structural coherence of the LAO films grown atop the STO substrates. Measurements of RSM around the (103) diffraction peaks for film and substrate reveal that the in-plane lattice parameter of the LAO layer is strained to that of STO. This demonstrates that LAO thin films grow pseudomorphically on STO substrates.

Transport measurements reveal that these heterostructures have a typical sheet resistance  $R_S$  between 10 and 30 k $\Omega$ /square at room temperature. Most of the samples display a small photoelectric effect ( $\Delta R/R < 5\%$ ) under ambient light illumination. As shown in figure 2(a), resistance measurements indicate a metallic behavior down to 4 K, with a residual resistivity ratio of the order of 25. Figure 2(b) displays the inverse sheet Hall constant as a function of temperature for the same sample. Considering a single band model, we estimate a sheet carrier density of the order of  $7 \times 10^{13}$  electrons  $\text{cm}^{-2}$

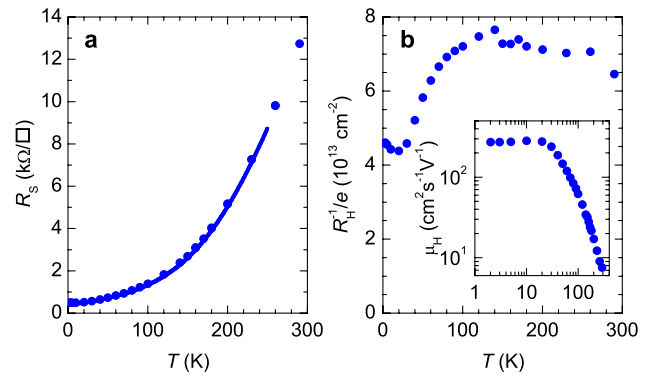


**Figure 2.** Transport properties in the normal state for an LAO/STO structure. (a) Sheet resistance as a function of temperature for a 4 u.c. thick LAO film grown onto a (001) STO substrate. The continuous line represents the resistance measurement during the cooling while the dots are measurements performed stabilizing the temperature during the heating cycle. (b) Inverse sheet Hall constant and mobility (inset) versus temperature for the same sample.

above 100 K. From sample to sample, the sheet carrier density varies between  $0.4$  and  $1.2 \times 10^{14}$  electrons  $\text{cm}^{-2}$ , without correlation with the thickness of the LAO layer. As can be noted in the figure, below 100 K, the inverse sheet Hall constant decreases as the temperature is reduced. Such a behavior has previously been observed in Nb-doped SrTiO<sub>3</sub> thin films [13] and attributed to multiband conduction. Although this issue is still controversial, it is known that doped SrTiO<sub>3</sub> possesses three degenerate bands for Ti 3d electrons [14]. This degeneracy is lifted by the structural phase transition occurring at  $\sim 105$  K. The inset of figure 2(b) shows the mobility versus temperature, which reaches a value of  $\sim 300$   $\text{cm}^2 \text{V}^{-1} \text{s}^{-1}$  at low temperatures.

Measurements of the resistance at low temperatures reveal that this electron gas condenses into a superconducting state. Figure 3(a) shows the sheet resistance versus temperature for a 4 u.c. thick LAO film. As can be seen, a superconducting transition occurs at a temperature of  $\sim 220$  mK. From magnetotransport measurements with the magnetic field

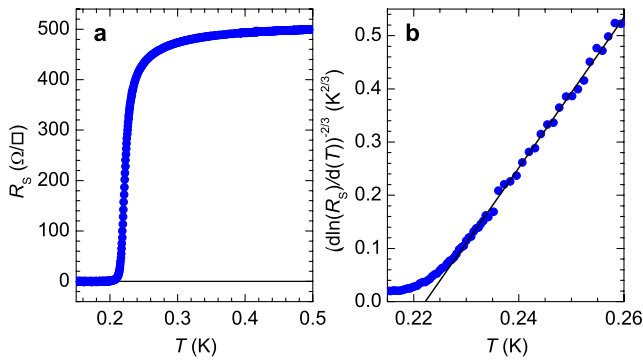


**Figure 3.** Transport properties at low temperatures. (a) Sheet resistance versus temperature for a 4 u.c. sample. (b)  $(d \ln R_S/dT)^{-2/3}$  versus temperature, revealing the linear behavior expected for a BKT transition: the extrapolation of the linear part to zero resistance leads to an estimate for  $T_{\text{BKT}}$  of about 222 mK.

applied perpendicular to the interface, we have estimated  $H_{c2}(0\text{ K})$  to be  $\sim 90$  mT [6], which leads to a superconducting coherence length  $\xi(0)$  of about 60 nm. As the thickness of the electron gas is below 10 nm [6, 11], we expect the system to behave as a 2D superconductor possibly with footprints of a Berezinskii–Kosterlitz–Thouless (BKT) transition [15, 16].

In the BKT scenario, the resistance as a function of temperature is expected to follow the relation  $R = R_0 \exp[-b(T/T_{\text{BKT}} - 1)^{-1/2}]$ , where  $T_{\text{BKT}}$  is the BKT transition temperature and  $b$  a material dependent parameter. To estimate  $T_{\text{BKT}}$  and  $b$  we rewrite the expression as  $(d \ln R/dT)^{-2/3} = (2/b)^{2/3}(T - T_{\text{BKT}})$ . This form has the advantage that  $b$  and  $T_{\text{BKT}}$  can be estimated from the characteristic linear behavior above  $T_{\text{BKT}}$ , without having to determine  $R_0$ . This analysis is shown in figure 3(b), where we notice that the resistance measurements are consistent with the BKT behavior. The rounding of the transition at the lowest temperatures is attributed to a size effect. The linear extrapolation to  $R = 0$  leads to  $T_{\text{BKT}} = 222$  mK.

#### 4. Conclusion

We have discussed the growth and characterization of LAO films grown onto (001) STO TiO<sub>2</sub>-terminated substrates. With the preparation conditions described above, we observe that only structures with an LAO thickness greater than 3 u.c. are

conducting. We have shown that the electron gas present at these LAO/STO interfaces condenses into a superconducting state displaying properties expected for a 2D superconductor.

#### Acknowledgments

We thank Anna-Sabina Ruetschi, Didier Jaccard, Jochen Mannhart, Toni Schneider and Marc Gabay for useful discussions and Marco Lopes for his technical assistance. We acknowledge financial support by the Swiss National Science Foundation through the National Center of Competence in Research ‘Materials with Novel Electronic Properties’ MaNEP and Division II, by the European Union through the project ‘Nanoxide’ and by the European Science Foundation through the program ‘Thin Films for Novel Oxide Devices’.

#### References

- [1] Ohtomo A and Hwang H Y 2004 *Nature* **427** 423
- [2] Okamoto S and Millis A 2004 *Nature* **428** 630–3
- [3] Hwang H Y 2006 *Mater. Res. Soc. Bull.* **31** 28–35
- [4] Bousquet E, Dawber M, Stucki N, Lichtensteiger C, Hermet P, Gariglio S, Triscone J M and Ghosez P 2008 *Nature* **452** 732–6
- [5] Brinkman A, Huijben M, van Zalk M, Huijben J, Zeitler U, Maan J C, van der Wiel W G, Rijnders G, Blank D H and Hilgenkamp H 2007 *Nat. Mater.* **6** 493–6
- [6] Reyren N, Thiel S, Caviglia A D, Kourkoutis L F, Hammerl G, Richter C, Schneider C W, Kopp T, Ruetschi A S, Jaccard D, Gabay M, Muller D A, Triscone J M and Mannhart J 2007 *Science* **317** 1196–9
- [7] Caviglia A D, Gariglio S, Reyren N, Jaccard D, Schneider T, Gabay M, Thiel S, Hammerl G, Mannhart J and Triscone J M 2008 *Nature* **456** 624
- [8] Nakagawa N, Hwang H Y and Muller D 2006 *Nat. Mater.* **5** 204–9
- [9] Thiel S, Hammerl G, Schmehl A, Schneider C W and Mannhart J 2006 *Science* **313** 1942–5
- [10] Reyren N 2009 *Appl. Phys. Lett.* at press
- [11] Basletic M, Maurice J L, Carrétéro C, Herranz G, Copie O, Bibes M, Jacquet E, Bouzehouane K, Fusil S and Barthélémy A 2008 *Nat. Mater.* **7** 621–5
- [12] Rijnders G, Koster G, Blank D H A and Rogalla H 1997 *Appl. Phys. Lett.* **70** 1888–90
- [13] Takahashi K S, Gabay M, Jaccard D, Shibuya K, Ohnishi T, Lippmaa M and Triscone J M 2006 *Nature* **441** 195–8
- [14] Mattheiss L F 1972 *Phys. Rev. B* **6** 4740
- [15] Berezinskii V L 1972 *Sov. Phys.—JETP* **34** 610
- [16] Kosterlitz J M and Thouless D J 1972 *J. Phys. C: Solid State Phys.* **5** L124